temperatures was not observed. The individual particles were also less regular of habit. At 70°C only hematite particles of diameters varying from 20 nm to 50 nm were present in a structureless flocculated state. At 85°C the diameter of the precipitated hematite is a function of α_o. The particular size decreases from 60 nm to 70 nm at α_o = 0.06 to about 15 nm at α_o = 0.20.

Van der Woude and de Bruyn (III.11) made what they believed to be the first evaluation of the activation energy for nucleation. From the temperature dependence of an Arrhenius plot of the induction period, they calculated an activation of 47 $\pm$ 4 kJ/mol (11.2 kcal/mole). A plot of the temperature dependence of the growth rate (k_m) of the amorphous colloid produced an activation energy of 50 $\pm$ 5 kJ/mol (12 kcal/mole). For growth the activation energy was stated to be low, on the order of the dehydration energy. Thus, the activation energy for nucleation and growth was about the same magnitude. It was pointed out that constant size of the amorphous particles implied a much closer relationship between the mechanisms of nucleation and growth than was expected from the classical treatment. The near constancy of the size of the amorphous phase regardless of the temperature and total iron(III) concentrations suggested that the critical nucleus must have a constant size not strongly dependent on supersaturation as would be the case in the classical treatment of nucleation. Dousma and de Bruyn (III.25) pointed out that the oxyhydroxide phase formed at room temperature stops growing once they reach the size range 20-40 A even after aging for more than one year.

Okamoto et al. (III.26) utilized Mössbauer spectroscopy to follow the phase changes of a gel prepared from iron(III) nitrate in a 1N NaOH solution at 100°C. The spectrum for a mixture aged for 4.5 hours is shown in Figure III.18. These authors

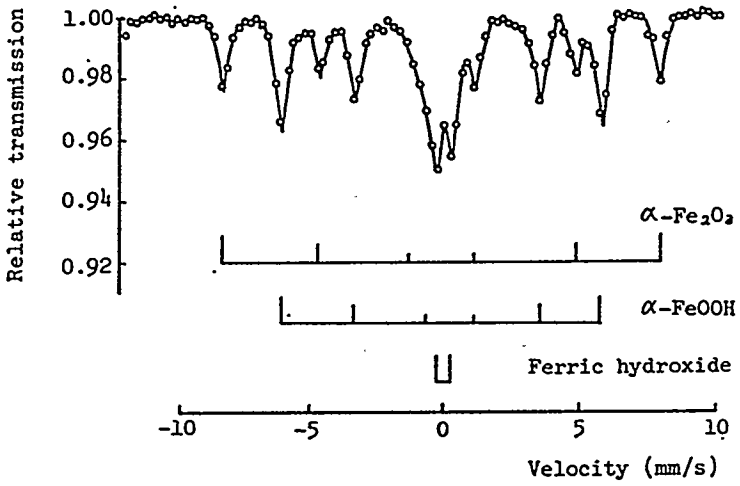

Figure III.18. Mössbauer absorption spectrum at room temperature of the sample aged in 1 N NaOH at 100°C for 4.5 hr (from reference III.26).

divided the reaction in three stages (Figure III.19): in the first stage the water content decreased with a marked increase in the saturation magnetization; in stage II α-Fe_2O_3 crystallized out which exhibited sharp X-ray diffraction lines indicating crystals larger

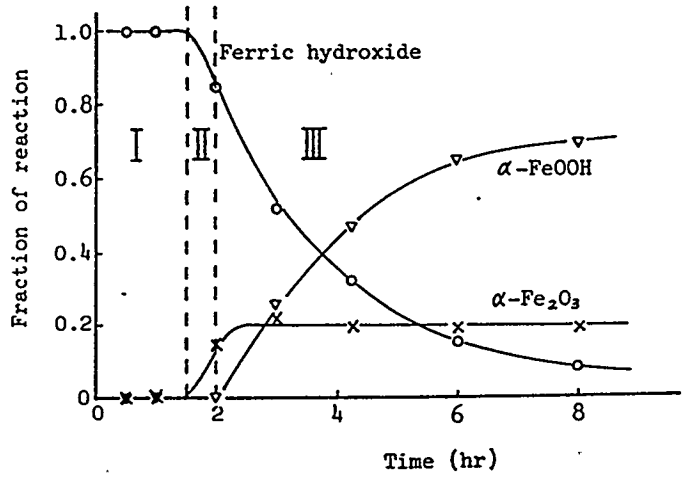

Figure III.19. Time dependence of the degree of phase changes from ferric hydroxide to α-Fe_2O_3 and α-FeOOH in 1 N NaOH solution at 100°C (from reference III.26).

than 0.1 μm and stage III where α-FeOOH crystals which were acicular were formed exclusively. Crystallization in 1NaOH and 1N $NaNO_3$ at 100°C was similar but the induction period increased remarkably.

III.C. β-FeOOH - Akageneite

A widely studied iron oxyhydroxide is β-FeOOH. Early interest in this material was developed because of the rather monodispersed spindle-shaped (cigar-type) particles of tetragonal crystal structure (III.27 - III.35). These sols have a unique particle structure consisting of tubular parallel rods (III.27 - III.29, III.36, III.37).

Sols of exceedingly small, but apparently uniform particles of ferric hydroxide, were obtained by Spiro et al. (III.38).

Matijević (III.39) showed that monodispersed sols could be repeatedly prepared by aging at elevated temperatures highly acidic solutions of ferric salts in the presence of sulfate ions. The resulting colloidal particles were well-defined basic ferric sulfates, whose size and shape depended on the experimental conditions. Furthermore, a comprehensive analysis of all solute species in solutions, from which the dispersions were generated, made it possible to define complexes responsible for the solid phase formation, suggesting chemical mechanisms of basic ferric sulfate precipitation (III.40).

Matijević and Scheiner (III.41) made a detailed study of the hydrothermal aging for times ranging from a few hours to a few weeks of sols prepared from nitrate, chloride or perchlorate solutions. They compared the solubility domains and the nature of the precipitate obtained from the three salts (Figures III.20, III.21, III.22).

Matijević and Scheiner utilized three different procedures in the preparation of ferric hydrous oxide dispersions: (a) addition of base to ferric salt solutions; (b) heating of such solutions in the absence or in the presence of base; and (c) adding an oxidizing agent to a ferrous salt solution and subsequent precipitation with base or

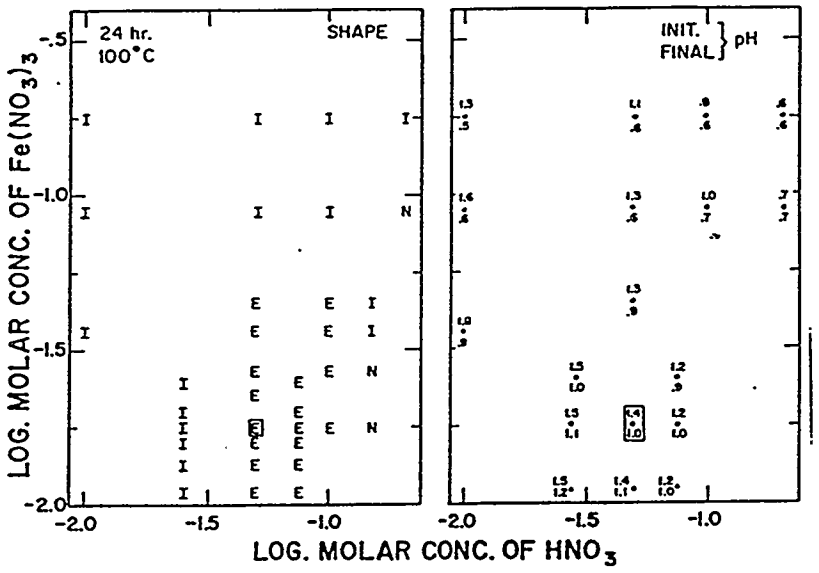

Figure III.20. Concentration domains of solutions containing $Fe(NO_3)_3$ and HNO_3 which were aged 24 hr at 100°C. Left side symbols: N, no precipitation; E, ellipsoidal shaped particles; I, irregular particles of varying sizes. Right side indicates initial (upper number) and final (lower number) pH of several studied systems (from reference III.41).

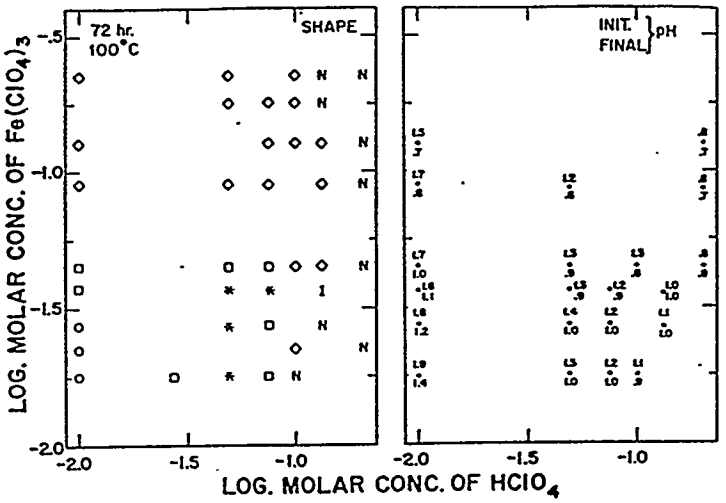

Figure III.21. Concentration domains of solutions containing $Fe(ClO_4)_3$ and $HClO_4$ which were aged 72 hr at 100°C. Left side symbols: N, no particle formation; Particle shapes: ◇, ellipsoidal; □, hexagonal and rhombic; *, bipyramidal; ○, spherical; I, irregular of varying sizes. Right side indicates initial (upper number) and final (lower number) pH of several studied systems (from reference III.41).

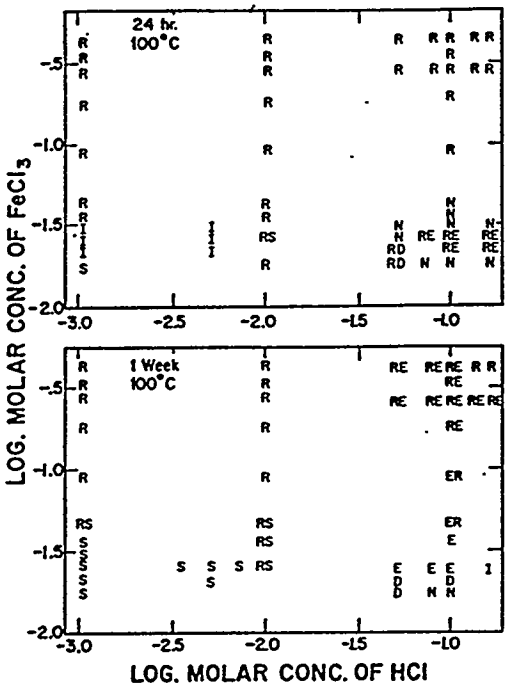

Figure III.22. Concentration domains of solutions containing $FeCl_3$ and HCl aged at 100°C for 24 hr (upper) and for 1 week (lower). Symbols: N, no particle formation. Particle shapes: D, double ellipsoid; E, ellipsoidal; I, irregular of varying sizes; R, rod-like; S, spherical. Pairing of symbols indicates a mixture of corresponding particles in the suspension. Particle composition: R, β-FeOOH; all other particles, α-Fe_2O_3 (from reference III.41).

by heating (or both). The composition of the solid phase depends in a most sensitive way on the conditions of the experiment, which include the concentrations and the nature of all species in solution, pH, temperature, rate and duration of heating, and postprecipitation treatment. Solutions of identical chemical composition can yield particles of different shape, size, or even different stoichiometry, if just one parameter is altered, e.g., time or temperature of aging. This explains, according to these authors, why some authors have offered domains which show changes in the nature of ferric hydrous oxide precipitates as a function of systematic variation in certain experimental conditions (III.32, III.42). Finally, the precipitates are not necessarily

stable products and can often rather easily change, both chemically and morphologically, as a result of postprecipitation treatment of the systems.

Despite all of this, Matijević and Scheiner (III.41) report that specific ferric hydrous oxides tended to form under certain conditions. For example, on addition of base amorphous ferric hydroxides are generated which, on aging, tend to crystallize either to α-FeOOH or to α-Fe_2O_3, depending on temperature (III.43). α-FeOOH or α-Fe_2O_3 may directly precipitate on heating solutions of ferric salts with anions other than chloride, if the pH is properly adjusted (III.44; Section III.B).

The effect of anions on the nature of the ferric hydr(oxide) precipitates was recognized early (III.45, III.46). Acidic solutions of $FeCl_3$ yield on aging most frequently β-FeOOH (III.27, III.35, III.42). The latter solid contains different concentrations of chloride ions, which are exchangeable. In the presence of sulfate ions, alunite type particles precipitate (III.39, III.40, III.42).

Matijević and Scheiner showed that a variety of rather uniform colloidal dispersions could be prepared by forced hydrolysis at elevated temperatures of *highly acidic* ferric salt solutions. The particle size and shape depended on the concentrations of the ferric salts and of the corresponding acids. Under these conditions the dominant composition of the particles was α-Fe_2O_3, although the particle shapes varied considerably. The latter depended on the anion present in the solutions which was aged. As an exception, some of the systems precipitated in ferric chloride solutions consisted of rod-like β-FeOOH. However, depending on conditions, ferric chloride solutions also produced α-Fe_2O_3, but the particle morphology was then

different. The β-FeOOH precipitates prevailed on short aging (24 hr., III.29), whereas on prolonged heating fewer systems consisted of acicular solids characteristic of this composition. Instead, particles of different shapes having the structure of α-Fe_2O_3 resulted. The cases of transformation of β-FeOOH to α-Fe_2O_3 were reported earlier (III.46 - III.48). It was also shown that β-FeOOH particle suspended in water undergo transformation to α-Fe_2O_3 at elevated temperatures much more readily than when kept in the air (III.48). In view of dissimilar structures such structural changes appeared to proceed through a renucleation process (III.47).

It is likely that in cases other than those involving β-FeOOH, α-FeOOH forms first and subsequently recrystallizes to α-Fe_2O_3. The latter process is irreversible but rather common due to the similarity of the structure.

Parida (III.49) prepared a number of β-FeOOH samples by varying the initial pH, quantity of urea and temperature of agitation. This method of generating a base in-situ has been labeled a homogeneous precipitation technique. It was observed at 100°C, using 50 g Fe^{3+}, 50 g urea and initial pH 1.52, that a precipitate formed in 15 min. and was complete in 6.5 hours. Conditions and properties of 11 samples obtained using this procedure are provided in Table III.4.

Table III.4

Methods of Preparation of Akaganeite Samples
and their Density and the Surface Area (from reference III.49)

Sample No.	Initial pH of Solution	Temperature of Preparation (°C)	Quantity of Urea (g)	Time of Hydrolysis (h)	Surface area (m^2/g^{-1})
1	1.52	100	50	6.5	20.22
2	1.52	100	100	3.5	23.86
3	1.52	100	150	2.5	24.03
4	1.52	100	200	1.5	31.65
5	0.6	100	200	20	14.41
6	1.05	100	100	4	28.22
7	1.90	100	50	4.5	50.10
8	1.52	85	100	11	26.50
9	1.52	70	200	40	21.01
10	1.52	60	250	140	19.86
11	0.4	85	200	45	18.90

The chloride content of these samples varied between 5 and 8.5 wt.%. The surface area of these samples is lower than for many of those materials described earlier.

Maeda and Hachisu (III.37) have examined β-FeOOH by electron microscopy. An aged sol containing particles 3500 A long and 600 A thick was placed in an observation cell and the water evaporated over 1-4 months (otherwise the structure was broken). They observed an interesting arrangement of particles (Figures III.23 and III.24) packed in a square lattice in the Schiller layers formed from the sols.

Davis (III.50) prepared a precipitate at a pH of about 7 by the addition of ammonium hydroxide to a $FeCl_3$ solution. The precipitate/colloidal dispersion was aged at room temperature for about 5 years. After this period the suspended solid consisted of particles about 3000 A long and 5-100 A in diameter; these particles were composed of a parallel arrangement of long "tubes". Aging for 10 more years resulted in no further crystal growth or change in crystal shape.

Figure III.23. The arrangement of β-FeOOH particles in the plane of smectic layer. Square cross section of the particle is producing square lattice (from reference III.37).

Figure III.24. The smectic layers are standing nearly perpendicularly to the bottom surface in a noniridescent area of the schiller layers (from reference III.37).

III.D. γ-FeOOH

The formation of γ-FeOOH from iron(II) compounds has been described (III.51). In this case the reaction requires oxidation and the process is complex. It has been proposed that FeOOH proceeds through intermediate species named Green Rusts (see Section III.F.).

The Green Rust that is formed depends upon the anions present in the solution. Green Rust I is reported to form when $FeCl_2$ was used as the starting material while Green Rust II was produced when $FeSO_4$ was used. The oxidation of dilute iron(II) in perchloric acid solution leads to an intermediate complex that approximates a stoichiometry of $[Fe(III)]_3[Fe(II)]$ (III.52). Magnetic susceptibility measurements data and Raman spectra were used to formulate a tetranuclear complex containing octahedral Fe(II) with three oxo Fe(III) bridges in the coordination sphere.

Air oxidation of neutral or slightly alkaline $FeSO_4$ solution was reported to produce a solid Green Rust II whose composition is [Fe(III)][Fe(II)] (III.53). It was reported that dilute solutions of the intermediate, Green Rust I or II, could be transformed into Fe_3O_4 by slow oxidation, or into γ-FeOOH by rapid air oxidation.

The mechanism for conversion of γ-FeOOH to Fe_3O_4 and Green Rust II has also been described (III.54). The conversion was studied in the presence of Fe(II) and SO_4^{2-} without any oxidation process. The transformation involves dissolution of γ-FeOOH by surface adsorption of Fe(II) (2 mol) on γ-FeOOH to produce a dissolved intermediate. The dissolved intermediate yields Green Rust II and Fe_3O_4. The

dissolved intermediate has the composition $[(Fe^{2+})_2(Fe^{3+})(OH^-)_4(O^{2-}]^+$, which upon reaction with sulfate ion yields Green Rust II.

Barton et al. (III.55) made a recent study in which they compared the product from air oxidation of $FeSO_4$ or $FeCl_2$ solutions with the product when either ethylenediaminetetraacetic acid (EDTA) or diaminocyclohexanetetraacetic acid was added to the sulfate solution.

The FeOOH crystals were grown from a 0.4 M $FeSO_4$ solution at 25°C. Either ethylenediaminetetraacetic acid or diaminocyclohexanetetraacetic acid was added as a solution in an amount sufficient to give a concentration of 0.01 M in a 1.5 liter reaction mixture. The acid was allowed to equilibrate for 10 min. in the Fe(II) solution. Sufficient sodium hydroxide solution was added to give an $OH^-:Fe^{2+}$ molar ratio of 2:1. During the 5 hr reaction the pH changed from 7.3 to 3.9. Oxygen flow at 0.12 cm^3/s was passed through the resulting Fe(II) hydroxide suspension. Agitation and dispersion were accomplished with a high shear stirrer.

During the course of oxidation 100 mL samples were removed from the reaction mixture. These samples were immediately centrifuged for 1 min. which allowed half of the solution volume to be decanted as a clear solution from the settled suspension. Gelatin was mixed in a 1:1 ratio with the centrifuged iron hydroxide material, then spread as a film onto an aluminum foil. After hardening 1 min. the film was pressed on a glass slide, and placed in a desiccator which had been purged with nitrogen. X-ray diffraction (XRD) measurements were made on the gelatin films.

Intermediate sampling was carried out for three $FeSO_4$ reactions, and one reaction in which $FeCl_2$ was used as the Fe(II) source. Of the three $FeSO_4$ reactions, one contained no growth modifier, one reaction contained 0.01 M EDTA, and one reaction contained 0.01 M DACHTA. The $FeCl_2$ reaction contained no growth modifier. Samples were removed at reaction times: 0, 60, 100, 180 and 300 min. for reaction with a 300 min. total oxidation time. Reaction times were measured from the beginning of oxygen flow.

An XRD pattern was obtained for a glass slide packed with gelatin in which no iron oxide was mixed. There is a noticeable hump in the background in the pattern due to scatter from the amorphous material (Figure III.25). For the reaction containing $FeSO_4$ with no growth modifier, the 60 min. sample showed strong peaks at 8°, 16°, and 24° 2θ which correspond to the [00z] reflections of Green Rust II. For the 100 min. sample, the intensity of these same reflections were greatly increased (Figure III.25). The intensity of the same three peaks was reduced for the 180 min. sample, and a small peak near the 100% peak at 21° 2θ for α-FeOOH was evident. In the XRD peaks for the 300 min. sample, peaks corresponding to Green Rust II were not detected, and only peaks for α-FeOOH remained. The influence of sulfate ion on the formation of Green Rust II compares with that reported earlier by Misawa et al. (III.53).

In the oxidation reaction of $FeCl_2$, the XRD pattern for the 60 min. sample had peaks at 8° and 11.5° indicating a mixture of Green Rust I and Green Rust II in a ratio of approximately 2:1 (Figure III.26). In the 100 min. sample, the ratio of Green Rust I

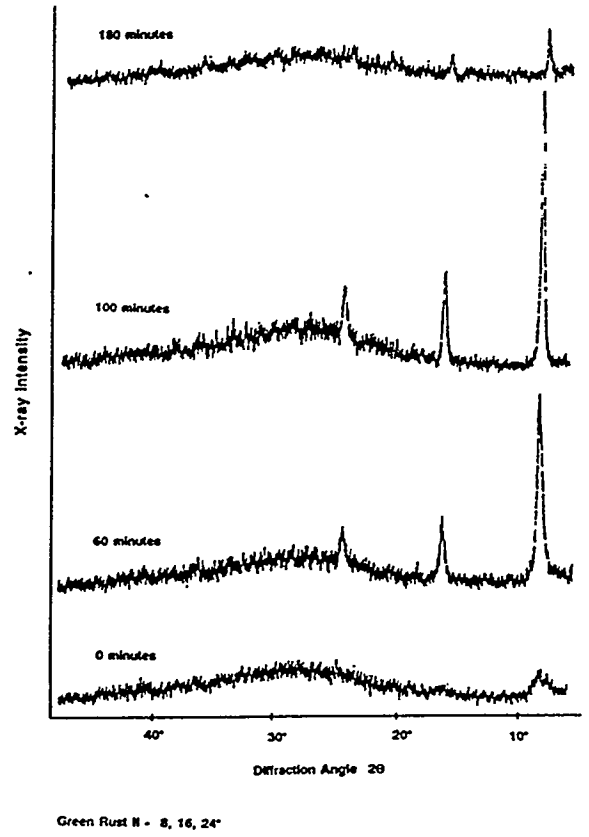

Figure III.25. XRD patterns for intermediate samples: preparation of α-FeOOH from $FeSO_4$ (from reference III.55).

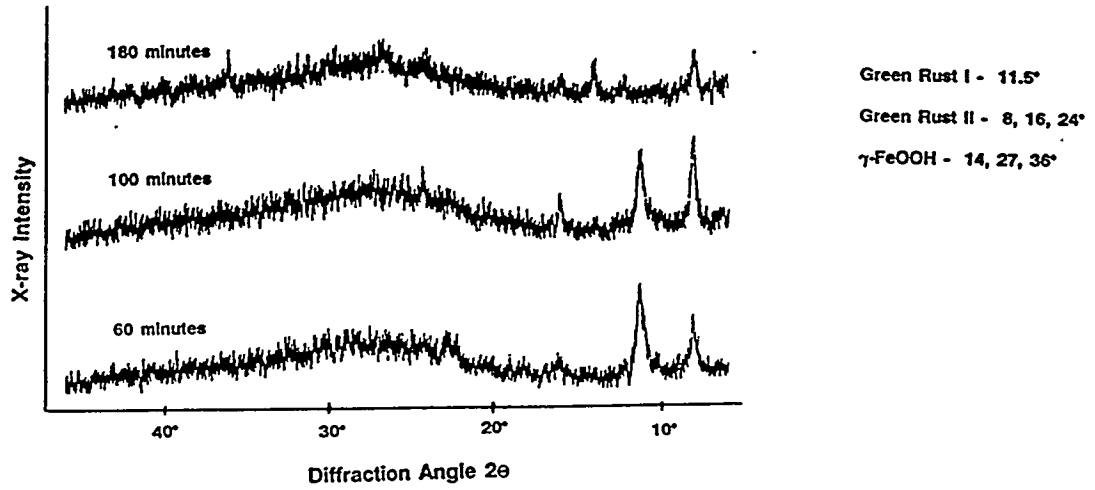

Figure III.26. XRD patterns for intermediate samples: preparation of γ-FeOOH from $FeCl_2$ (from reference III.55).

to Green Rust II was approximately 1:1. For the 180 min. sample, no Green Rust I was detected, a small amount of Green Rust II was present, and peaks for γ-FeOOH were evident. Bernal et al. (III.51) found the same two intermediate species during the oxidation of $FeCl_2$. Their conclusion was that Green Rust I contained mostly Fe^{2+} and some Fe^{3+}, with hydroxide, water and chloride ion comprising the rest of the composition. As further oxidation occurred, Green Rust I was converted to Green Rust II, which was thought to be made up of Fe^{2+} and Fe^{3+}, with a greater Fe^{3+} concentration, and with no chloride coordination. Various compositions for Green Rusts have been suggested. The chemical composition was not evaluated in the study by Barton et al. (III.55).

For the oxidation of $FeSO_4$ in the presence of EDTA, an XRD pattern for the 60 min. sample showed strong peaks corresponding to the [00z] planes of Green Rust II, and no evidence of Green Rust I (Figure III.27). The XRD pattern for the 100 min. sample (Figure III.27) contained very strong reflections from the [00z] planes of Green Rust II, and reflections from other planes, either from Green Rust II or any other intermediate species, were not detected. For the 180 min. sample the intensity of Green Rust II reflections had diminished greatly, and a peak at 14° 2θ from γ-FeOOH was found. Only reflections due to γ-FeOOH were evident in the sample collected at 300 min.

The samples removed from the reaction containing 0.01 M DACHTA had XRD patterns similar to those for samples removed from the reactions containing 0.01 M EDTA. The product of the reaction in 0.01 M DACHTA at 25°C was 100% γ-FeOOH.

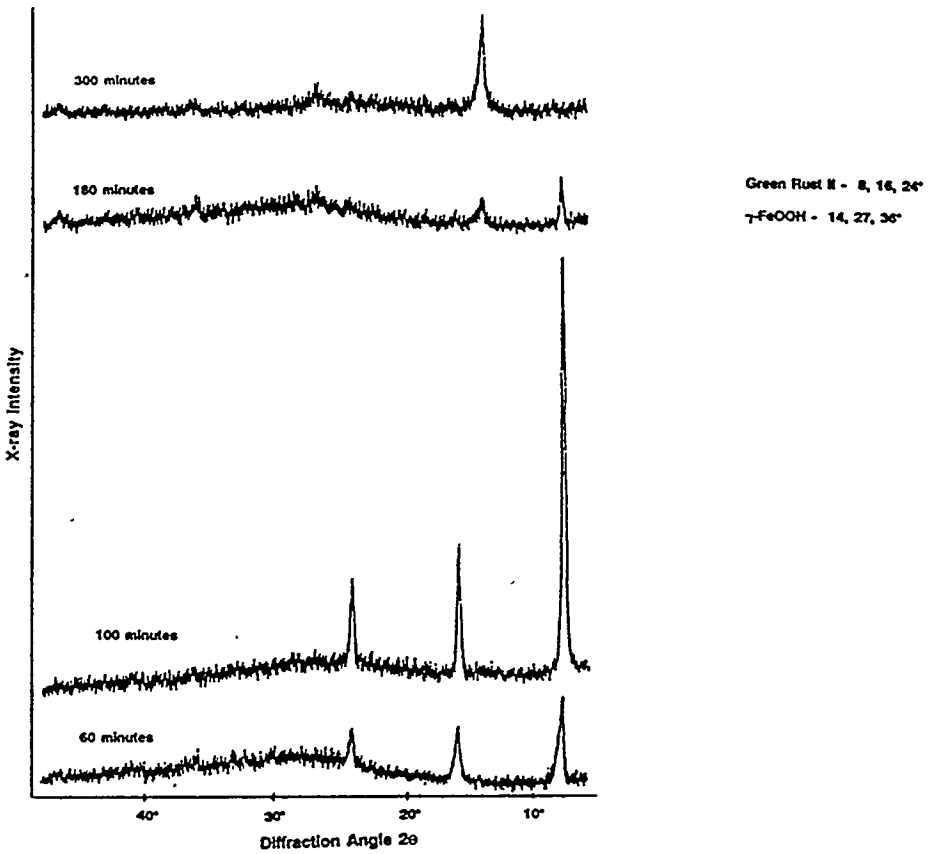

Figure III.27. XRD patterns for intermediate samples: preparation of γ-FeOOH from 0.4 M $FeSO_4$ in the presence of 0.01 M EDTA at 25°C (from reference III.55).

EDTA and DACHTA act in a similar manner to produce γ-FeOOH from $FeSO_4$. During the formation of α-FeOOH, and during the formation of γ-FeOOH in the presence of these growth modifiers, the only detectable crystalline intermediate phase is Green Rust II. The peaks in the XRD pattern corresponding to the [001], [002], and [003] are strongest in the 100 min. sample removed from both reactions, indicating that the crystal lattice is well formed along the z axis of Green Rust II. The axis transforms to the long axis in the needle-like crystals of α-FeOOH and γ-FeOOH prepared from these reactions.

The absence of non-[00z] reflections of Green Rust II in the intermediate samples may indicate a lack of significant lattice formation in the x and y directions in the mixed iron hydroxide species. This finding suggests that the action of EDTA and DACHTA is to induce the formation of γ-FeOOH from $FeSO_4$ and that this may be by alteration of the Green Rust II lattice in the x and y directions. The γ-FeOOH crystals prepared under these conditions are approximately twice as long, with length to width aspect ratios twice as large as for α-FeOOH crystals grown under the same conditions but without EDTA or DACHTA (III.56). The action of EDTA and DACHTA as growth modifiers seems to be as inhibitors of crystal growth in the x and y directions of Green Rust II, which allows preferential growth along the z axis. The coordination of these growth modifiers along the z backbone structure alters the iron-oxygen bonds in such a way that the γ-FeOOH lattice is favored over the α-FeOOH lattice. Previous work by Barton et al. (III.56) showed that EDTA addition after 100 min. of reaction time for an oxidation process requiring 300 min., led to the formation only of α-FeOOH rather than γ-FeOOH. Addition of EDTA before 80 min. of reaction time produced γ-FeOOH. It is within this time frame that the reflections of Green Rust II are most intense. The conclusion drawn from this evidence is that EDTA alters Green Rust II as it forms. After all Green Rust II is formed, the conversion to FeOOH occurs. Only Green Rust II that has been altered by coordination with EDTA leads to γ-FeOOH. Nonaltered Green Rust II transforms to α-FeOOH under these conditions. The mode EDTA or DACHTA coordination to the Green Rust II intermediate is not known.

Barton et al. (III.56) studied the impact of the amount of EDTA addiditives as well as the influence of the time during the course of the reaction when it was added. When sodium hydroxide was added to a ferrous sulfate solution at 40°C, and oxygen was flowed through the resulting hydroxide suspension, the product after 5 hr. was a viscous yellow slurry of α-FeOOH. The addition of EDTA to the reaction mixture prior to the oxidation produced at the end of the 5 hr. reaction an orange slurry. X-ray powder diffraction patterns shown in Figure III.28 determined that the orange crystals were γ-FeOOH.

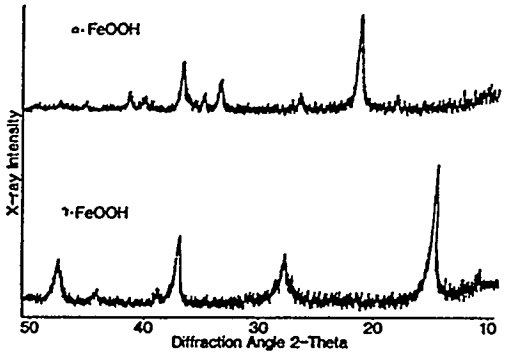

Figure III.28 X-ray powder diffraction patterns of α-FeOOH grown with no EDTA, and γ-FeOOH grown from $FeSO_4$ in the presence of EDTA (from reference III.56).

Subsequent experiments at various concentrations of EDTA carried out at 40°C showed that below 0.0025 M EDTA, the amount of γ-FeOOH formed was below the 5 vol.% detection limit of XRD (Figure III.29). When EDTA solution concentrations

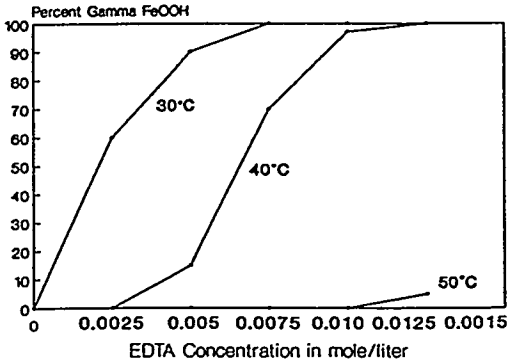

Figure III.29. Graph of the dependence of γ-FeOOH production on EDTA concentration (from reference III.56).

between 0.005 and 0.0125 M EDTA were used, a mixture of α-FeOOH and γ-FeOOH was formed. An estimation of the amount of each phase produced was made by ratioing the 100% peaks for γ-FeOOH and α-FeOOH in the XRD spectra. At EDTA solution concentrations above 0.0125 M, 100% γ-FeOOH was produced. This concentration dependence was found to be significantly influenced by the temperature of the reaction. At 50°C, approximately 5% by volume γ-FeOOH was formed using 0.0125 M EDTA. At 30°C, a 0.0075 M EDTA solution was sufficient to produce 100% γ-FeOOH. Transmission electronmicrographs show that γ-FeOOH particles produced at 40°C with 0.0125 M EDTA are uniform needle-like crystals approximately 800 nm long (Figure III.30). Crystals produced at 25°C with 0.0075 M EDTA were smaller with an approximate length of 600 nm. The lower temperature changes the kinetics of

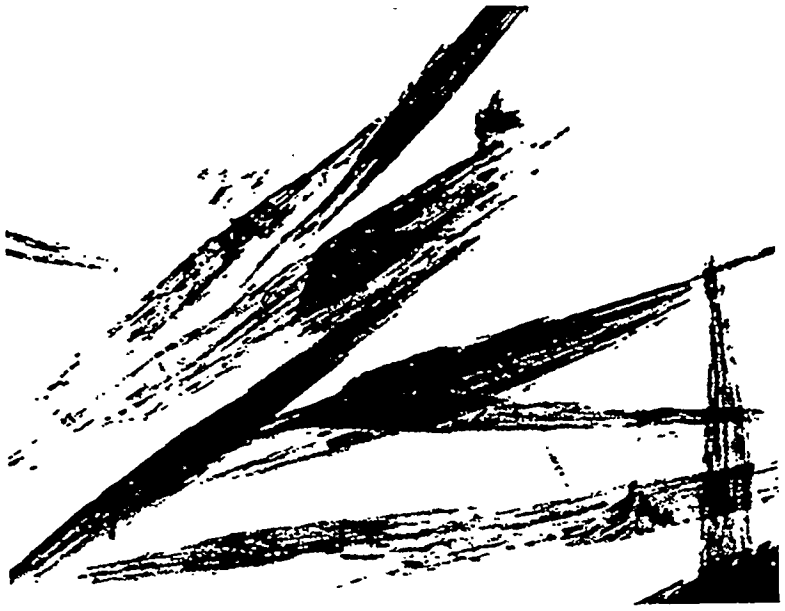

Figure III.30. Transmission electron micrograph taken at 28,000 X magnification of bundles of γ-FeOOH crystals grown with EDTA (from reference III.56).

γ-FeOOH growth, although it is the oxygen flow rate that is the limiting factor in the rate of conversion from $Fe(OH)_2$ to FeOOH. The oxygen use is so fast using the high shear stirring apparatus that no bubbles are seen rising to the surface of the reaction vessel even at relatively high oxygen flow rates. Reactions at 40 and 25°C also take 5 hr. to complete conversion of Fe(II) to Fe(III) at the fixed oxygen flow rate.

Photoacoustic infrared spectra of the products of the EDTA reactions show bands that correspond to γ-FeOOH.

The experiments in which EDTA was added at different times during the oxidation reaction were designed to investigate how EDTA affected the mechanism of FeOOH nucleation and growth. Addition of 0.0125 M EDTA to the reaction mixture before 1 hr. and 20 min. produced nearly 100% γ-FeOOH at 40°C. A small peak near the 100% peak for α-FeOOH may indicate a small fraction of that phase at a concentration near the lower detection limit of XRD. Addition of 0.0125 M EDTA after 1 hr. and 40 min., however, produced essentially 100% α-FeOOH (Figure III.31). This

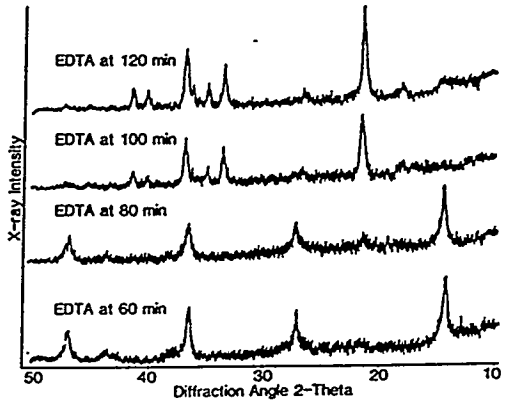

Figure III.31. X-ray powder diffraction patterns of the products from variable time EDTA addition reactions (from reference III.56).

time-dependent behavior indicated that the influence of EDTA may be as a nucleating agent and suggested that nucleation of FeOOH occurs only in a time period between

1 hr. and 20 min., and 1 hr. and 40 min. of reaction time at this rate of oxidation. Assuming a constant oxidation rate, the species that exist during the period of nucleation should have an Fe(III):Fe(II) ratio of approximately 1:3. Barton et al. (III.56) consider the fact that nucleation occurs in a window supports work by Misawa et al. (III.57), who describe the oxidation of Fe(II) to Fe(III) as proceeding via a series of chain structures of Fe(II) and Fe(III). Barton et al. concludes that it does not appear that individual Fe(III) atoms formed new discrete nuclei of FeOOH after initiation of nucleation. Rather, all Fe(III) produced after the initiation time was added to the growing crystals. An Fe(III):Fe(II) ratio of 1:3 during this nucleation period indicates that the phase of the resulting crystal is fixed before the green rust (II) stage, which has been assigned an Fe(III):Fe(II) ratio of 1:2 by Mackey (III.59).

To elucidate the mechanism by which EDTA nucleated the γ-FeOOH phase, Barton et al. utilized model compounds of EDTA as additives in the synthetic schemes.

These authors selected compounds that would contain functional groups that may be involved in the EDTA iron interactions in producing γ-FeOOH; the compounds utilized were:

EDTA and Compounds Selected for Study as Models in the Production of γ-FeOOH from $FeSO_4$

Ethylenediaminetetraacetic acid (EDTA)
$(HO_2CCH_2)_2NCH_2CH_2N(CH_2CO_2H)_2$

Ethylenediaminediacetic acid (EDDA)
$(HO_2CCH_2)NHCH_2CH_2NH(CH_2CO_2H)$

Ethylenediamine
$H_2NCH_2CH_2NH_2$

Iminodiacetic acid (IDA)
$NH(CH_2CO_2H)_2$

Pyromellitic acid (PMA)

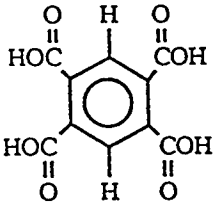

Ethylenediaminetetramethylenephosphonic acid (EDTMPA)
$[(OH)_2OPCH_2]_2NCH_2CH_2N[CH_2PO(OH)_2]_2$

IDA resembles either end of EDTA because of the amine species centered between two acetate groups; this grouping alone does not appear sufficient to induce the production of γ-FeOOH. PMA contains four carboxylic acid groups held at a fixed distance by a rigid ring; only α-FeOOH was produced in the presence of this compound showing that either the distance between the acid groups in PMA differs from that of EDTA or the four carboxylic acid groups alone are not a sufficient condition. Ethylenediamine produced only α-FeOOH. EDDA, which contains a single carboxylic acid group attached to each nitrogen atom, produced essentially pure α-FeOOH. EDTMPA is similar in structure to EDTA but contains phosphoric acid groups instead of carboxylic acid groups; this compound produced tiny amorphous particles of iron oxide with small amounts of α-FeOOH.

Naono and Nakai (III.59) investigated the formation and thermal decomposition of γ-FeOOH using a procedure similar to one used by Kiyama and coworkers (III.60). After 61 g of $FeCl_2$ was dissolved in 1.0 dm^3 of 0.24 N HCl, the solution was neutralized by 1.0 N NaOH solution and diluted with distilled water to 2.0 dm^3. In the experiment, 0.5 g of $Na_2HPO_4 \cdot 2H_2O$ was added to the suspension to prevent formation of α-FeOOH nuclei. The neutral suspension (pH = 7) was deep blue. By bubbling air (500 dm^3/hr) at 10-15°C, the color of the suspension changed from deep blue via green to orange yellow, showing a decrease of pH from 7 to 4. The period of air oxidation was 2-3 hr. γ-FeOOH nuclei thus formed were grown at 50°C, where the pH of the suspension was kept almost at 4 by adding 1.0 N NaOH solution dropwise. Four samples were prepared under the different growth periods.

Naono and Nakai (III.59) observed that the growth of γ-FeOOH nuclei formed in acidic medium showed that in the initial stage a number of ultrafine needle crystallites 50 A wide are grown from the central part of the nuclei to both sides along the c axis of γ-FeOOH. As growth continues the gap between needle crystallites is gradually filled. As growth continues a flat surface appears and finally acicular fine particles having well-developed (010) surface are formed. The appearance of the (010) surface has been claimed by a number of authors for both mineral and synthetic lepidocrocite, γ-FeOOH (III.61 - III.65). XRD confirmed that the crystal structure formed in the presence of phosphate was quite pure γ-FeOOH. With the growth of the particles, the diffraction intensity of (020) or (120) peaks, i.e., (hkl) peaks for $l = 0$, increases more rapidly compared with that of (031) or (002) peaks, i.e., (hkl) peaks for $l \neq 0$. This leads to the conclusion that the γ-FeOOH particles grow preferentially along the c axis of γ-FeOOH, and this result is consistent with the morphological observation based upon TEM pictures.

A γ-FeOOH sample aged for 19 hours was utilized in measurements of Kr adsorption. For materials with a surface that is predominately flat surfaces, a step or steps will be observed in the lower pressure regions of the adsorption isotherm (Figure III.32). As the γ-FeOOH is decomposed by heating the step in the isotherm disappears.

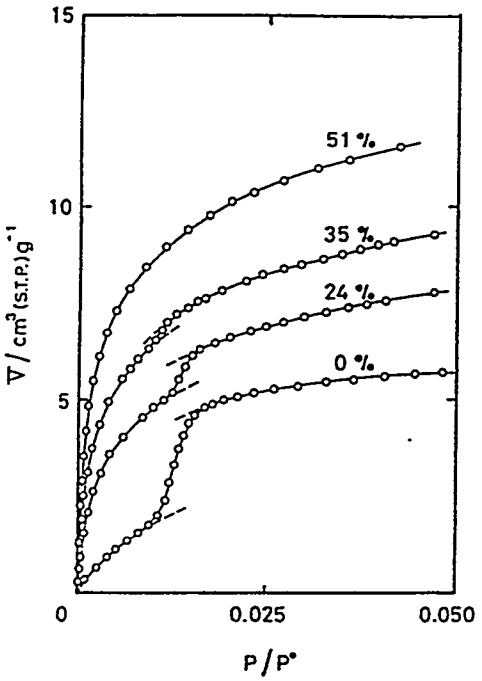

Figure III.32. Adsorption isotherms of Kr gas at various degrees of decomposition of Sample D. Figures given are the degree of decomposition of γ-FeOOH (from reference III.59).

III.E. δ-FeOOH

Francombe and Rooksby (III.66) showed that the compound identified by Glemser and Gwinner (III.67) as δ-Fe_2O_3 was in fact δ-FeOOH. They based their contention on an analysis of the X-ray data. Bernal et al. (III.69) also identified the material prepared by Glemser and Gwinner as δ-FeOOH. The material is produced by the very rapid oxidation of an Fe(II) with an excess of a concentrated solution of hydrogen peroxide or ammonium persulfate. However, if the oxidation is carried out in a dilute solution of hydrogen peroxide or ammonium persulfate added slowly, γ-Fe_2O_3 can be formed from $Fe(OH)_2$. If oxygen is passed slowly through a strongly alkali suspension of $Fe(OH)_2$ one produces α-FeOOH. Thus, only the procedures involving lower temperatures and rapid oxidation lead to δ-FeOOH.

Olowe et al. (III.69) prepared two samples of δFeOOH by adding a sufficient quantity of hydrogen peroxide to cause the violent oxidation of a ferrous hydroxide suspension. Two ratios, R, of $[Fe^{2+}]i/[OH^-]$ were used: R = 0.2 and R = 0.4. The initial precipitate of ferrous hydroxide (0.2 M in each case) was aged for about 1 hour prior to addition of hydrogen peroxide. The sample obtained for R = 0.2 has a disc-like shape and has XRD and electron diffraction patterns resembling what Olowe et al. call α'-FeOOH. The sample obtained at R = 0.4 shows that the majority of crystals are thin hexagonal platelets of δ-FeOOH with mean diameter varying from about 300 A to about 1520 A. These crystal sizes are larger than those generally reported in the literature (III.57; III.58; III.70-III.72). These results suggest that the crystal size of δ-FeOOH strongly depends on the method of preparation and the ratio R.

III.F. Mechanism of Oxidation of Ferrous Hydroxide - Green Rusts and their Transformation

Olowe (III.73) made a detailed study of the mechanism of the oxidation of iron(II) under a range of conditions as well as the transformations occurring for intermediate products. While the studies were directed toward understanding the mechanism of iron corrosion, they provide general understanding that is applicable to catalyst preparation. Olowe paid special attention to the structures of Green Rust I and II (GR1 and GR2), as well as their formation and transformations.

The presence of certain anions like CO_3^{2-}, NO_3^-, Cl^-, Br^-, SO_4^{2-}, etc., has been found to influence, depending on the electrode potential and the pH of the solution, the oxidation mechanism of ferrous hydroxide which might lead to the formation of

intermediate compounds containing ferrous and ferric ions in different proportions. Two such transient compounds have been identified in solutions containing simple or planar anions like CO_3^{2-}, Cl^- or Br^- and in solutions containing SO_4^{2-} ions; they are classified (III.47), based on their X-ray diffraction patterns, as Green Rust 1 (GR1) and Green Rust 2 (GR2), respectively.

Olowe (III.73) achieved the simulation of each oxidation process by stirring, in the presence of air, a mixture of different concentrations of melanterite ($FeSO_4 \cdot 7H_2O$ and caustic soda (NaOH). One hundred milliliters of a predetermined concentration of melanterite was prepared and poured in a 400 mL beaker; an equal volume of another predetermined concentration of caustic soda was prepared separately, and mixed gradually with the melanterite in which the agitator was already in motion.

The experimental arrangement used has a major advantage over others described in literature, in that a direct and thus continuous measurement of the electrode potential (E_h) and pH with time is made. In parallel, a direct recording of the variation of E_h with pH is also made using another X-Y recorder. Thus, the advance of the oxidation process is clearly identified and followed. These curves have been found very useful in the evaluation of several parameters of the kinetics, and in the preparation of specific samples like pure GR2. Calomel is used as reference electrode for both the measurement of E_h and pH. The value of E_h is measured with respect to a platinum electrode.